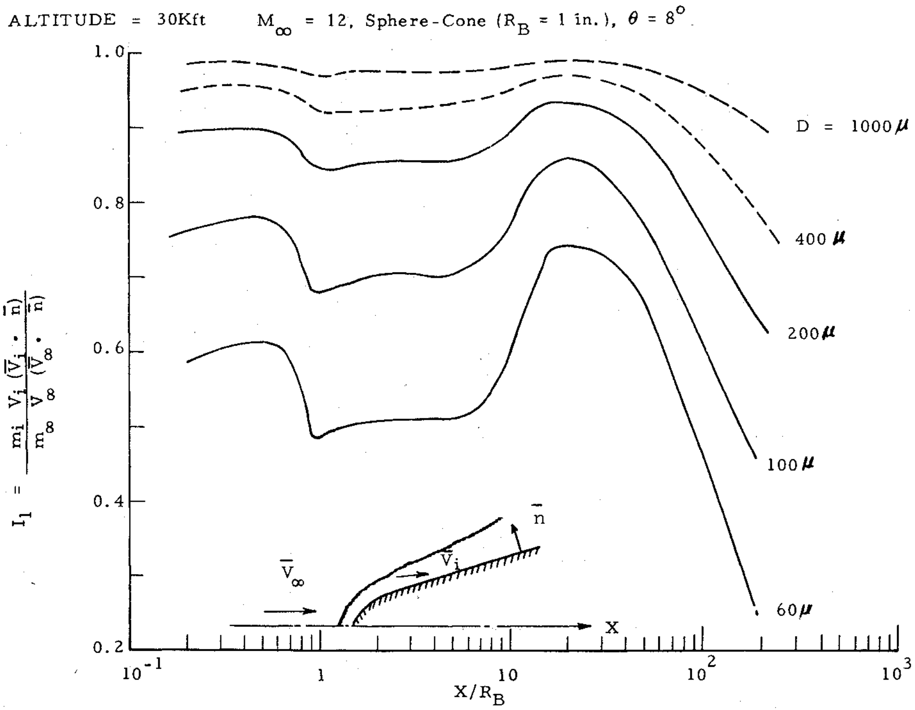

Fig. 6 Ice-crystal kinetic energy impact ratio on blunt cone: spherical ice particle.

The statistical particle size distribution function for ice crystals can be represented by an exponential relation.[1] The net kinetic energy impact fraction at the stagnation point then becomes

$$\Lambda = \int_0^\infty \frac{m_i u_i^2}{6m_\infty u_\infty^2} \zeta^3 \exp(-\zeta) d\zeta, \quad \zeta = \frac{D}{6.06D_S}$$

where m_∞ represents ambient particle mass, subscript i denotes conditions at impact, and D_S is a reference particle diameter.[1] Figure 5 shows the variation of Λ with D_S for a 2.8-in. body cylinder radius. Numerical results for spherical ice particle impact downstream of the stagnation region are shown in Fig. 6. Here we have considered a sphere-cone body geometry with a cone half-angle of 8 deg. For the larger ice particles, the trajectory deflection and slow-down attributable to shock layer effects is insignificant and can be neglected. For the smaller ice crystals ($D < 200$ μ), the shock layer becomes an effective shielding mechanism in decelerating the particle. It is interesting to note that a minimum appears in $I_l = m_i V_i (\bar{V}_i \cdot \bar{n}) / m_\infty V_\infty (\bar{V}_\infty \cdot \bar{n})$ near the cone-sphere junction.§ Far downstream (e.g., $X/R_B > 25$), I_l starts to decrease due to the thickening of the shock layer. This behavior of I_l is associated principally with the increase in the particle deflection angle.

In Ref. 13, we have considered the questions of the spinning of ice particles, the effects of thermal shock, and the problem of high-temperature radiant energy transfer. It was concluded that the thermal shock effects and the tumbling of the cylindrical ice particles are not important because of the small-particle residence time. A large angular velocity is induced, however, which may cause the ice to crack or break up.

References

[1] Waldman, G. and Reinecke, W., "Particle Trajectory, Heating and Breakup in Hypersonic Shock Layers," *AIAA Journal*, Vol. 9, June 1971, pp. 1040-1048.

[2] Probstein, R. F. and Fassio, F., "Dusty Hypersonic Flows," *AIAA Journal*, Vol. 8, April 1970, pp. 772-779.

[3] Wu, P.K.S., "Advanced Reentry Aeromechanics," Physical Sciences, Inc., Wakefield, Mass., PSI-TR-10, Aug. 30, 1974.

[4] Bethe, H. A. and Adams, M. C., "A Theory for the Ablation of Glassy Materials," *Journal of the Aerospace Sciences*, Vol. 26, June 1959, pp. 321-358.

§Here I_l represents the shock-layer shielding effect on ice-crystal kinetic energy impact ratio.

[5] Pappas, C. C. and Lee, G., "Heat Transfer on a Hypersonic Blunt Cone with Mass Addition," *AIAA Journal*, Vol. 8, May 1970, pp. 954-956.

[6] Lewis, C. H., Adams, J. C., and Gilley, G. E., "Effects of Mass Transfer and Chemical Nonequilibrium on Slender Blunted Cones," ARO, Inc., Tullahoma, Tenn., AEDC-TR-68-214, Nov. 1968.

[7] Lees, L., "Similarity Parameters for Surface Melting of a Blunt Nosed Body in a High Velocity Gas Stream," *ARS Journal*, Vol. 29, May 1959, pp. 345-354.

[8] Jaffe, N. A., "Droplet Dynamics in a Hypersonic Shock Layer," *AIAA Journal*, Vol. 11, Nov. 1973, pp. 1562-1564.

[9] Fay, J. A. and Riddell, F. R., "Theory of Stagnation Point Heat Transfer in Dissociated Air," *Journal of the Aerospace Sciences*, Vol. 25, Feb. 1958, p. 73.

[10] Liu, T. M., "3-D Inviscid Flow Analysis," Avco System Div., Wilmington, Mass., AVSD-0335-74-RR, Dec. 1974.

[11] Bailey, A. B. and Hiatt, J., "Free-Flight Measurements of Sphere Drag," ARO, Inc., Tullahoma, Tenn., AEDC-TR-70-291, March 1971.

[12] Hoerner, S. F., "Fluid Dynamic Drag," published by the author, 1958.

[13] Lin, T. C. and Thyson, N., "Investigations of Ice Crystals in the Shock Layer of a High Speed Vehicle," Avco Systems Div., Wilmington, Mass., Avco TR-K210-74-17, Sept. 1974.

[14] Carlson, D. J. and Hoglund, R. F., "Particle Drag and Heat Transfer in Rocket Nozzles," *AIAA Journal*, Vol. 12, Nov. 1963, pp. 1980-1984.

Heat Transfer in Wall Jet Flows with Vectored Surface Mass Transfer

Rama Subba Reddy Gorla*
Cleveland State University, Cleveland, Ohio

Nomenclature

C_f = local skin friction coefficient
E = Eckert number $U^2/cp\ (T_w - T_\infty)$
f = nondimensional stream function

Received Feb. 14, 1977; revision received April 25, 1977.
Index categories: Boundary Layers and Convective Heat Transfer—Laminar; Thermal Control.

*Associate Professor, Department of Mechanical Engineering.

g = ξ-derivative of f
h = ξ-derivative of g
K = transformed tangential surface velocity
k = thermal conductivity
Nu = Nusselt number
Pr = Prandtl number
q = heat flux
Re = Reynolds number
T = temperature
U = characteristic velocity
u = velocity component in streamwise direction
v = velocity component in transverse direction
x = coordinate along streamwise direction
y = coordinate normal to the surface
η = nondimensional coordinate
θ = nondimensional temperature
ν = kinematic viscosity
ξ = transformed mass-transfer parameter
ρ = density
ϕ = ξ-derivative of θ
χ = ξ-derivative of ϕ
ψ = stream function

Subscript
w = conditions at the wall

Introduction

THE flow pattern that results when a jet of fluid is discharged tangentially along a plane surface is called a plane wall jet. Wall jet flows are used in many practical situations. Some of these are in boundary-layer control, metal ingot cooling, paper drying, gas turbine blade cooling, window deicing, glass tempering, etc.

The effect of the surface mass transfer boundary condition in a plane wall jet is to introduce nonsimilarity in the velocity field. The nonsimilarity in the velocity field makes the thermal problem nonsimilar. In a recent study, Gorla[1] analyzed the effect of uniform mass transfer at the wall in a normal direction. Series as well as local nonsimilarity solutions were presented in Ref. 1, to study the flow and heat-transfer characteristics. The present work is undertaken to provide local nonsimilarity solutions for the flow and heat transfer in a plane wall jet with vectored mass transfer along the surface such that v_w is uniform along the surface and $u_w \sim x^{-1/2}$. These particular distributions of wall velocities are chosen because they allow the integration to proceed in an ordinary way. In fact, they result from an examination of the continuity equation in conjunction with the stream function at the wall.

Analysis

For a laminar, steady, incompressible, two-dimensional flow, where the viscosity coefficient remains constant and pressure gradient, body forces, and viscous dissipation are negligible, the governing equations within boundary-layer approximation are given by the following:

Mass:

$$\partial u/\partial x + \partial v/\partial y = 0 \tag{1}$$

Momentum:

$$u(\partial u/\partial x) + v(\partial u/\partial y) = \nu(\partial^2 u/\partial y^2) \tag{2}$$

Energy:

$$u(\partial T/\partial x) + v(\partial T/\partial y) = \alpha(\partial^2 T/\partial y^2) \tag{3}$$

where x and y are the distances measured along and normal to the surface, respectively, u and v are the corresponding velocity components, and T is the temperature. The boundary conditions are given by

$$y=0 : u=u_w, \quad v=v_w, \quad \text{and} \quad T=T_w \tag{4a}$$

$$y\to\infty : u=0 \quad \text{and} \quad T=T_\infty \tag{4b}$$

Positive and negative values for v_w imply blowing and suction, respectively.

Proceeding with the analysis, we define

$$\psi = (\nu^3 U)^{1/4} x^{1/4} f(\xi,\eta) \tag{5a}$$

$$\eta = (1/4)(U/\nu)^{1/4} x^{-3/4} y \tag{5b}$$

$$\xi = 4v_w (x^3/\nu^3 U)^{1/4} \tag{5c}$$

$$\theta = (T-T_\infty)/(T_w - T_\infty) \tag{5d}$$

$$u_w = (K/4)(U\nu/x)^{1/2} \tag{5e}$$

The case of isothermal wall boundary condition will be discussed in this Note. The momentum and energy equations, together with the corresponding boundary conditions, can be written as

$$f''' + ff'' + 2[f']^2 = 3\xi\left[f'\left(\frac{\partial^2 f}{\partial\eta\partial\xi}\right) - f''\left(\frac{\partial f}{\partial\xi}\right)\right] \tag{6}$$

$$f + \xi = -3\xi(\partial f/\partial\xi) \quad \text{at} \quad \eta = 0 \tag{7a}$$

$$f'(\xi,0) = K \qquad f'(\xi,\infty) = 0 \tag{7b}$$

$$(1/Pr)\theta'' + f\theta' = 3\xi\left[f'\left(\frac{\partial\theta}{\partial\xi}\right) - \theta'\left(\frac{\partial f}{\partial\xi}\right)\right] \tag{8}$$

$$\theta(\xi,0) = 1 \qquad \theta(\xi,\infty) = 0 \tag{9}$$

Primes denote differentiation with respect to η.

Equations (6-9) do not admit a similarity solution, and so the local nonsimilarity method has been used. Since the methods of deriving the various levels of local nonsimilarity models have been well documented in literature,[2,3] these details will not be given here in the interest of conserving space. The present work employed the third level of truncation model. To this end, we define

$$g = \frac{\partial f}{\partial\xi}, \qquad h = \frac{\partial g}{\partial\xi}, \qquad \phi = \frac{\partial\theta}{\partial\xi}, \qquad \chi = \frac{\partial\phi}{\partial\xi}$$

and then write the governing equations for the third level of truncation model as follows:

Velocity Problem

$$f''' + ff'' + 2f'^2 = 3\xi(f'g' - f''g) \tag{10}$$

$$g''' + fg'' + 4f''g + f'g' = 3\xi[(g')^2 + f'h' - g''g - f''h] \tag{11}$$

$$h''' + fh'' + 8gg'' + 7f''h - 2f'h' - 2(g')^2 = 0 \tag{12}$$

Boundary conditions

$$f(\xi,0) = -\xi/4 \quad f'(\xi,0) = K \quad f'(\xi,\infty) = 0$$

$$g(\xi,0) = -1/4 \quad g'(\xi,0) = 0 \quad g'(\xi,\infty) = 0$$

$$h(\xi,0) = 0 \quad h'(\xi,0) = 0 \quad h'(\xi,\infty) = 0 \tag{13}$$

Thermal Problem

$$(1/Pr)\theta'' + f\theta' = 3\xi[f'\phi - g\theta'] \tag{14}$$

$$(1/Pr)\phi'' + f\phi' + 4g\theta' - (3f'\phi) = 3\xi[g'\phi + f'\chi - h\theta' - g\chi'] \tag{15}$$

$$(1/Pr)\chi'' + f\chi' + 8g\phi' + 7h\theta' - 6f'\chi - 6g'\phi = 0 \tag{16}$$

Boundary conditions

$$\theta(\xi,0) = 1 \quad \theta(\xi,\infty) = 0 \quad \phi(\xi,0) = 0$$

$$\phi(\xi,\infty) = 0 \quad \chi(\xi,0) = 0 \quad \chi(\xi,\infty) = 0 \tag{17}$$

The local wall shear stress is given by

$$\frac{\tau w}{\rho} = \nu \frac{\partial u(x,y)}{\partial y}\bigg)_{y=0} = \frac{1}{16}\left[\frac{\nu^5 U^3}{x^5}\right]^{1/4} f''(\xi,0) \tag{18}$$

If one defines

$$Re_x = Ux/\nu \text{ and } C_f = \tau w / [(\rho U^2)/2]$$

then Eq. (18) can be rewritten as

$$C_f (Re_x)^{5/4} = f''(\xi,0)/8 \tag{19}$$

The local wall heat flux can be written as

$$q_w = -k\frac{\partial T(x,y)}{\partial y}\bigg)_{y=0} - u_w \tau_w = -\frac{k}{4}\left[\frac{U}{\nu x^3}\right]^{1/4}$$

$$\times (T_w - T_\infty)\theta'(\xi,0) - \frac{K}{64}\left[\frac{U^5 \mu^7}{x^7 \rho^3}\right]^{1/4} \cdot f''(\xi,0) \tag{20}$$

In the previous equation, $q_w < 0$ indicates heat transferred to the surface. The heat-transfer coefficient is given by

$$h(x) = q_w(x)/(T_w - T_\infty) \tag{21}$$

and so the Nusselt number becomes

$$Nu_x = h(x)x/k = -(1/4)Re_x^{1/4} \cdot \theta'(\xi,0)$$

$$-(K/64) \cdot Re_x^{-3/4} \cdot Pr.E.\ f''(\xi,0) \tag{22}$$

Discussion of Results

The governing equations for the third level of truncation have been solved numerically on the computer by means of a forward integration fourth-order Runge Kutta method. The values of ξ ranged from -0.8 to 0.8, whereas the tangential surface velocity K was allowed to vary from 0 to 0.75.

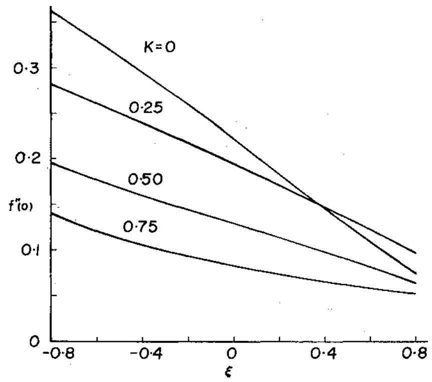

Fig. 1 Effect of downstream vectored surface mass transfer on local wall shear stress.

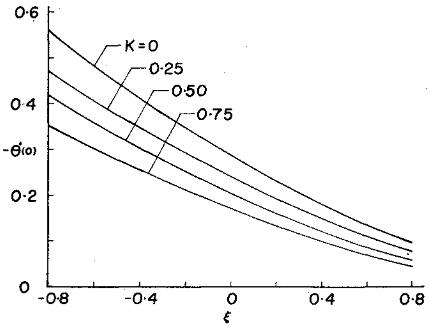

Fig. 2 Effect of downstream vectored surface mass transfer on local Nusselt number ($Pr = 0.73$).

Figure 1 shows curves for the local skin-friction coefficient vs ξ for downstream vectoring. It can be observed that the local wall shear decreases monotonically with ξ. The addition of streamwise momentum coupled with normal injection tends to increase the wall shear. This explains the crossing of the curves for positive values of ξ.

Figure 2 shows curves for the heat-transfer results for downstream vectored surface mass transfer. It is seen that the local Nusselt number decreases monotonically with ξ. The surface heat-transfer rate is observed to decrease with increasing values of K. A value of 0.73 has been used for the Prandtl number.

Acknowledgment

The author is grateful to a reviewer for some helpful remarks.

References

[1] Gorla, R. S. R., "Flow and Heat Transfer Characteristics of Wall Jets by the Method of Local Nonsimilarity," *Developments in Mechanics*, Vol. 8, March 1975, pp. 517-533.

[2] Sparrow, E. M., Quack, H., and Boerner, C. J., "Local Nonsimilarity Boundary Layer Solutions," *AIAA Journal*, Vol. 8, Nov. 1970, pp. 1936-1942.

[3] Sparrow, E. M. and Yu, H. S., "Local Nonsimilarity Thermal Boundary Layer Solutions," *Journal of Heat Transfer, Transactions of the ASME*, Vol. 93, Nov. 1971, pp. 328-334.

[4] Glauert, M. B., "The Wall Jet," *Journal of Fluid Mechanics*, Vol. 1, Dec. 1956, pp. 625-643.

[5] Gorla, R. S. R. and Jeng, D. R., "Laminar Plane Wall Jet," *Developments in Mechanics*, Vol. 6, Aug. 1971, pp. 137-151.

Goethert's Rule with an Improved Boundary Condition

Wilson C. Chin*

Boeing Commercial Airplane Company, Seattle, Wash.

Introduction

A GOETHERT rule is presented which identifies a linearized subsonic compressible flow with a family of affinely related exact incompressible flows. A modified transformation in the supersonic case casts the problem in hyperbolic canonical form, so that the results of Heaslet and Lomax[1] are directly applicable. The boundary conditions

Received April 12, 1977; revision received July 18, 1977.

Index categories: Aerodynamics; Supersonic and Hypersonic Flow; Subsonic Flow.

*Specialist Engineer, Aerodynamics Research Group.